

Methyl-Coenzyme M Reductase from Methanogenic Archaea: Isotope Effects on the Formation and Anaerobic Oxidation of Methane

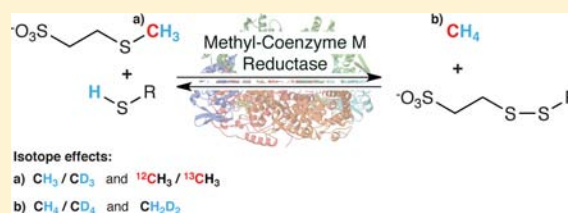
Silvan Scheller,^{†,§} Meike Goenrich,[‡] Rudolf K. Thauer,[‡] and Bernhard Jaun^{*,†}

[†]Laboratory of Organic Chemistry, ETH Zurich, Wolfgang-Pauli-Strasse 10, 8093 Zurich, Switzerland

[‡]Max Planck Institute for Terrestrial Microbiology, Karl-Von-Frisch-Strasse 10, 35043 Marburg, Germany

Supporting Information

ABSTRACT: The nickel enzyme methyl-coenzyme M reductase (MCR) catalyzes two important transformations in the global carbon cycle: methane formation and its reverse, the anaerobic oxidation of methane. MCR uses the methyl thioether methyl-coenzyme M ($\text{CH}_3\text{-S-CH}_2\text{CH}_2\text{-SO}_3^-$, Me-S-CoM) and the thiol coenzyme B (CoB-SH) as substrates and converts them reversibly to methane and the corresponding heterodisulfide (CoB-S-S-CoM). The catalytic mechanism is still unknown. Here, we present isotope effects for this reaction in both directions, catalyzed by the enzyme isolated from *Methanothermobacter marburgensis*. For methane formation, a carbon isotope effect ($^{12}\text{CH}_3\text{-S-CoM}/^{13}\text{CH}_3\text{-S-CoM}$) of 1.04 ± 0.01 was measured, showing that breaking of the C–S bond in the substrate Me-S-CoM is the rate-limiting step. A secondary isotope effect of 1.19 ± 0.01 per D in the methyl group of $\text{CD}_3\text{-S-CoM}$ indicates a geometric change of the methyl group from tetrahedral to trigonal planar upon going to the transition state of the rate-limiting step. This finding is consistent with an almost free methyl radical in the highest transition state. Methane activation proceeds with a primary isotope effect of 2.44 ± 0.22 for the C–H vs C–D bond breakage and a secondary isotope effect corresponding to 1.17 ± 0.05 per D. These values are consistent with isotope effects reported for oxidative cleavage/reductive coupling occurring at transition metal centers during C–H activation but are also in the range expected for the radical substitution mechanism proposed by Siegbahn et al. The isotope effects presented here constitute boundary conditions for any suggested or calculated mechanism.



INTRODUCTION

Methyl-coenzyme M reductase (MCR) catalyzes methane formation in all methanogenic archaea.¹ MCR is a 280 kDa enzyme built from three different protein chains in a C_2 -symmetric $\alpha_2\beta_2\gamma_2$ assembly with two active sites, each containing one molecule of the nickel hydrocorphinato F430 (Figure 1) as the prosthetic group.

The substrates of MCR are methyl-coenzyme M ($\text{CH}_3\text{-S-CoM}$), a methyl thioether, and coenzyme B (CoB-SH), a thiol, which are converted to methane and the heterodisulfide (CoM-S-S-CoB) according to Scheme 1.

Microbial communities carrying out the reverse process, the anaerobic oxidation of methane (AOM), have been discovered near methane seeps and on methane clathrates in the ocean.^{6,7} These communities consist of ANME-type archaea, which are genetically related to methanogens of the order *Methanomicrobiales* (ANME-1) and *Methanosarcinales* (ANME-2 and ANME-3), and of sulfate-reducing bacteria.² Together, they convert methane and sulfate to carbonate and hydrogen sulfide. Metagenomic analysis of the whole consortia indicated that the ANME archaea possess homologues of most of the genes associated with methanogenesis except those for hydrogenases.⁸ Accordingly, it is postulated that ANME archaea use essentially the same enzymes and pathways as the methanogens but in the

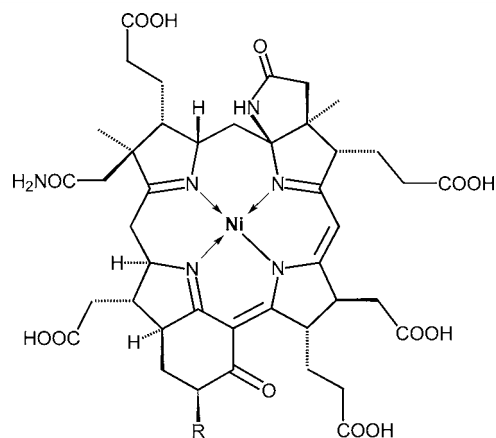


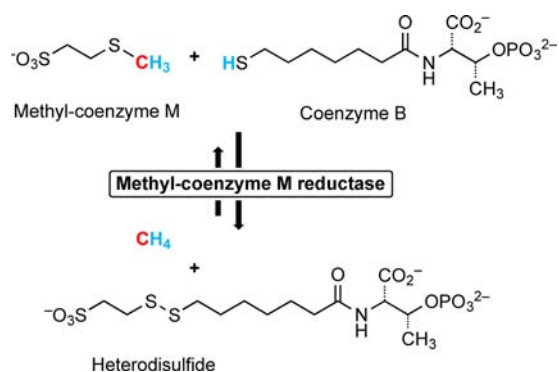
Figure 1. Factor F430, the prosthetic group of MCR. R = H for the cofactor found in methanogens and in ANME-2 and ANME-3 organisms.² R = S- CH_3 for the cofactor³ found in ANME-1.^{4,5}

reverse direction to oxidize methane. The first step in this sequence, the conversion of methane to methyl-coenzyme M,

Received: June 26, 2013

Published: September 4, 2013

Scheme 1. Reaction Catalyzed by Methyl-Coenzyme M Reductase (MCR)



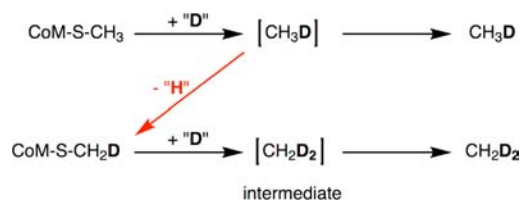
has recently been demonstrated to be catalyzed by MCR (isolated from a methanogen) at a rate comparable to that estimated for the AOM communities.⁹ Hence, methane formation and the anaerobic oxidation of methane are manifestations of one single catalytic mechanism driven in opposite directions. However, no precedent from non-enzymatic chemistry is available in either direction. Accordingly, the reaction mechanism remains still unknown, despite considerable effort by several research groups.^{1,10–13}

It is known that the nickel center of F430 must be in the Ni(I) oxidation state^{14,15} for the enzyme to be active. Accordingly, only strictly anaerobic harvesting of the cells and purification procedures yield active enzyme with >90% Ni(I), an extremely oxygen-sensitive species.¹⁶

Although X-ray structures are only available from inactive Ni(II) states, they reveal that the substrates have to enter the active site through a long narrow channel, which opens into an essentially hydrophobic cavity above the hydrocorphinoid plane of F430.^{17–19} This geometric setup is consistent with the ordered bi bi kinetics observed in the methane forming direction, where CH₃-S-CoM has to bind first, followed by CoB-SH.²⁰ The narrow entrance channel and the limited space inside the proximal dome may also contribute to the high specificity of the enzyme. CH₃CH₂-S-CoM is the only S-alkyl homologue of CH₃-S-CoM that serves as a substrate, but it is converted to ethane at a catalytic efficiency less than 1% of that of CH₃-S-CoM.^{18,19} With the homologous chiral substrate CH₃CDT-S-CoM, the stereochemical course of the reaction was shown to involve partial overall inversion,²¹ which will be discussed in more detail in the accompanying article (Scheller, S.; Goenrich, M.; Thauer, R. K.; Jaun, B. *J. Am. Chem. Soc.* 2013, 135, 10.1021/ja4064876).

Thus far, no intermediate has been observed spectroscopically when the active enzyme is incubated with its two natural substrates, neither by rapid quench methods nor in the steady state. However, we have recently reported evidence for the formation of at least one intermediate from isotope exchange into the substrate when the assays are run in deuterated buffer, as depicted in Scheme 2.²²

Since the fourth hydrogen of methane originally stems from the solvent,²³ the measurement of the primary H/D kinetic isotope effect on the C–H bond formation is a solvent isotope effect and has to be measured in a noncompetitive setup by comparing the initial rates of the reaction in H₂O and in D₂O. Because of the extreme oxygen sensitivity of active MCR and the low enzyme concentrations required to determine initial rates, this is a notoriously difficult experiment to carry out, and

Scheme 2. Methane Formation in Deuterated Medium Leads to Incorporation of Deuterium into Methyl-Coenzyme M (red arrow) via an Intermediate That Already Contains a Methane Molecule (drawn in brackets)^a

^aFormation of doubly labeled methane is the result of deuterium incorporation into the substrate.

thus far, our corresponding data only allow us to specify this solvent isotope effect as $k_{\text{H}_2\text{O}}/k_{\text{D}_2\text{O}} = 1.3 \pm 0.3$ with an upper limit of 1.6.^{24–26}

Here, we present studies of competitive isotope effects for both directions, the formation of methane from methyl-coenzyme M and the activation of methane to give methyl-coenzyme M.

RESULTS

Measurement of Isotope Effects on Methane Formation. Methane formation catalyzed by MCR involves at least one intermediate and thus two transition states, as described in the Introduction. Partitioning of the intermediate between forward reaction and reversal to substrate is temperature dependent with the highest forward commitment (25:1) found at the highest temperatures as shown by the data in Table 1. This observation in itself constitutes independent evidence for at least two transition states.

Table 1. Ratio of Methane Formation (overall reaction) to Isotope Exchange (reversibility of the first step) at ~50% Conversion^a

T [°C]	conversion to methane [%]	CH ₂ D-S-CoM in remaining substrate [%]	methane formed per CH ₂ D-S-CoM formed
4	44.5	8.6	9.3
22	54.7	7.3	16.6
40	54.2	5.4	22.1
60	45.9	3.4	24.8

^aAssays were run with 0.5 equiv of coenzyme B relative to methyl-coenzyme M; this limited conversion to ~50%, after which methane formation and D-incorporation into the substrate ceased.

Since the ratio of methane formed per substrate regenerated (as CH₂D-S-CoM) equals ~25 at 60 °C, the reversibility of the first step can be neglected when studying isotope effects on methane formation. Hence, the isotope effects measured for overall methane formation are very close to the intrinsic IEs for the first step, whereas potential isotope effects due to the second step are masked and cannot be quantified in this setup.

Carbon Isotope Effect on Methane Formation. The ¹²C/¹³C kinetic isotope effect on methane formation is measured in a competitive experiment by analyzing the remaining substrate at high conversion for the enrichment in the heavy label according to the method of Singleton.²⁷

A 1:1 mixture of ¹²CH₃-S-CoM/¹³CH₃-S-CoM is employed, and both the conversion to methane and the ¹³C/¹²C ratio in

the remaining substrate are determined by ^1H NMR spectroscopy of the crude assay solution (Figure 2).

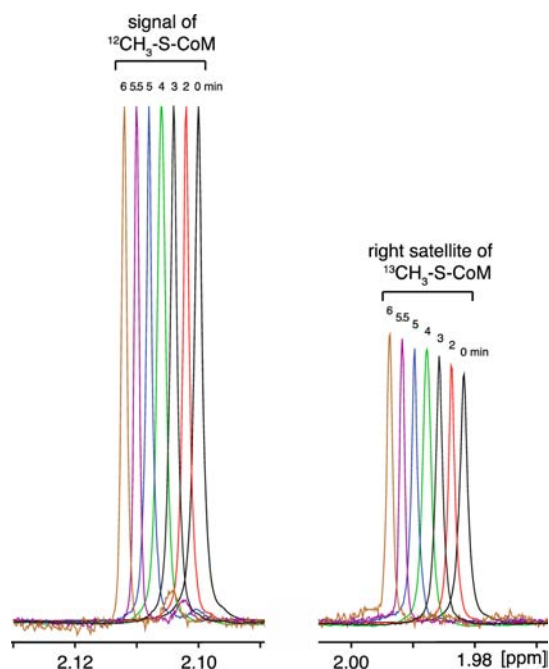


Figure 2. ^1H NMR (600 MHz) spectra of the centrifuged assay solution after 0, 2, 3, 4, 5, 5.5, and 6 min incubation with active enzyme at 60 °C. An assay with the reductant Ti(III)citrate was used in order to achieve high conversion to methane. The ppm scale refers to the spectrum at 0 min (black). Spectra for increasing times are plotted with a horizontal offset for better visibility. All spectra are adjusted to the same height for the signal due to $^{12}\text{CH}_3\text{-S-CoM}$.

Determination of the isotope effect is performed by analyzing the enrichment of the ^{13}C label according to the following equation:²⁸

$$\frac{R}{R_0} = (1 - F)^{1/\text{KIE}-1}$$

whereby F is the fraction of conversion, R_0 is the initial ratio of $^{13}\text{C}/^{12}\text{C}$ in the substrate, and R is the ratio of $^{13}\text{C}/^{12}\text{C}$ at conversion F .

The kinetic isotope effect is determined to be 1.039 ± 0.005 on the basis of an average of individual values obtained at six different fractions of conversion (see Supporting Information [SI], Table S1.3). The correlation of the conversion and the enrichment of the heavy isotope are plotted in Figure 3. To take into account the error in the measurement of the conversion, especially important at high conversions, the confidence interval was extended to ± 0.01 , giving $k_{12\text{C}}/k_{13\text{C}} = 1.04 \pm 0.01$, a substantial carbon isotope effect.

Secondary H/D-Isotope Effects on Methane Formation. The secondary isotope effects on methane formation ($\text{CH}_3\text{-}/\text{CD}_3\text{-S-CoM}$) are determined by analyzing the isotopologues of methane formed from a mixture of deuterium-labeled and undeuterated substrate (Table 2).

The average of the four experiments leads to a secondary kinetic IE of 1.187 ± 0.005 per D, assuming that this secondary isotope effect originates from the same transition state as the $^{12}\text{C}/^{13}\text{C}$ isotope effect.

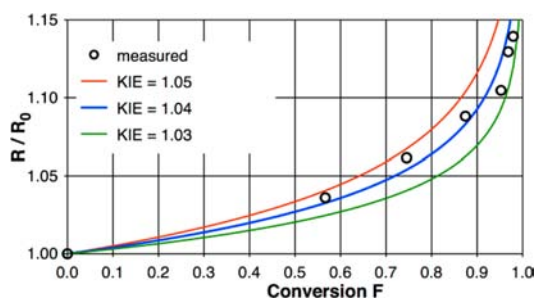


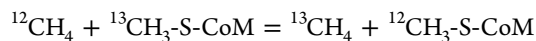
Figure 3. Enrichment of the ^{13}C -labeled substrate at high conversion due to the kinetic isotope effect. Blue: mean value determined. Red and green: boundaries of the extended confidence interval (see SI, S1.2).

Taking the (small) error in the measurement of the isotopic composition of the substrate into account, the resulting secondary isotope effect is $k_{\text{H}}/k_{\text{D}} = 1.19 \pm 0.01$ per D.

With a Ti(III)citrate assay, in which CoM-S-S-CoB is continuously reduced to CoM-SH and CoB-SH (see SI, S1.4 for details) a secondary isotope effect of 1.17 per D is obtained.

Procedure to Measure Isotope Effects on Methane Activation. The reverse reaction, the activation of methane, is endergonic ($\Delta G^{\circ} = 30 \pm 10 \text{ kJ mol}^{-1}$) and thus runs only until the thermodynamic equilibrium is reached, which corresponds to approximately 0.18% conversion with 5 mM heterodisulfide and 2 bar methane (see SI, S1.6 for details).

Equilibrium conditions, in which both substrates and both products of the reaction are present, allow observation of methane activation via $^{12}\text{C}/^{13}\text{C}$ label exchange from methane to methyl-coenzyme M⁹ according to the following net stoichiometry:



In order to measure isotope effects of methane activation, deuterium-labeled and unlabeled methane need to be activated, yielding labeled and unlabeled methyl-coenzyme M. The amount of Me-S-CoM formed equals the amount of methane activated.

Since the reaction sequence proceeds via an intermediate, putative label exchange from the solvent has to be investigated first. Three different pathways of label exchange are conceivable, exemplified here with D_2O as the solvent and unlabeled substrates and products (Scheme 3).

All three different pathways of label exchange (A, B, and C) are probed in the same experiment, in which methane activation is carried out in D_2O , and both the remaining methane in the headspace and methyl-coenzyme M in solution are analyzed for their isotopic composition.

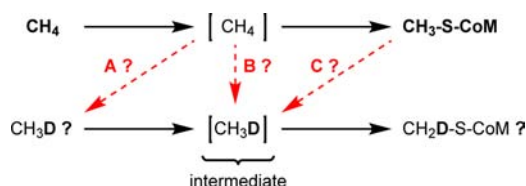
Methane Activation in Deuterated Medium, Shielding of the Active Site. D_2O buffer is used as the solvent, and methyl-coenzyme M is labeled with ^{13}C . Otherwise, the setup is the same as for the measurement of the rate of methane activation described previously.⁹ The isotopic composition of both the assay solution and the headspace is determined before addition of enzyme (0 min) and after incubation with active enzyme for 32 min at 60 °C (Table 3).

It can be deduced from the data in Table 3 (last column) that virtually no $^{12}\text{CH}_3\text{D}$ has been formed from the $^{12}\text{CH}_4$ employed, which rules out pathway A (deuterium incorporation into methane).²⁹

Table 2. Molar Fraction of Methane Isotopologues Formed from a Mixture of CD₃-S-CoM and ¹³CH₃-S-CoM^a

time [min]	¹³ CH ₄ [%]	CH ₂ D ₂ [%]	CHD ₃ [%]	ratio ¹³ CH ₄ /CHD ₂ L ^b	KIE ^c	KIE corr ^d	KIE per D ^e
Run 1							
2	56.14	1.66	42.20	1.280	1.615	1.677	1.188
4	55.97	1.53	42.49	1.271	1.604	1.666	1.185
Run 2							
2	55.83	1.75	42.43	1.264	1.594	1.656	1.183
4	56.30	1.58	42.12	1.288	1.625	1.688	1.191

^aCoenzyme B (0.2 equiv) was used relative to Me-S-CoM to limit the conversion to 20% and thus approach the measurement of relative initial rates. ^bL symbolizes H or D, CHD₂L equals the sum of CH₂D₂ and CHD₃. ^cValues for kinetic isotope effects (KIE) are corrected for the measured ratio of ¹³CH₃-S-CoM/CD₃-S-CoM = 44.22% / 55.78% in the substrate solution at *t* = 0 (see S1.3 in SI for details). ^dKIE corrected for the ¹³C KIE (values multiplied by 1.039). ^eCubic root.

Scheme 3. Three Putative Deuterium Exchange Pathways in Methane Activation^a

^a(A) Label exchange in the reaction of methane to the intermediate (partial reversibility), which would lead to deuteration of methane; (B) label exchange from the solvent into the intermediate, which would result in additional deuterium atoms found in the methyl-coenzyme M formed and in the methane employed; (C) label exchange in the substrate (already investigated for methane formation) taking place under the equilibrium conditions used for the activation of methane.

Table 3. Methane Activation under Equilibrium Conditions in Deuterated Buffer^a

species [nmol]	0 min ^b	32 min ^b	formed	formed from ¹² CH ₄
Solution				
¹³ CH ₃ -S-CoM	6334	2586		
¹³ CH ₂ D-S-CoM	2 ^c	413	411	
¹³ CHD ₂ -S-CoM	0 ^c	26	26	
¹² CH ₃ -S-CoM	64	384	320	320 ± 7
¹² CH ₂ D-S-CoM	0 ^c	6	6 ^d	2 ± 2
Headspace				
¹³ CH ₄	2199	2247	48	
¹³ CH ₃ D	1 ^c	2123	2122	
¹³ CH ₂ D ₂	0 ^c	249	249	
¹² CH ₄	197696	195241		
¹² CH ₃ D	104 ^c	140	36 ^e	15 ± 8

^aIsotopic composition of Me-S-CoM in the assay solution and of methane in the headspace gas are determined from one identical sample. Column 4 (“formed”) shows species formed during incubation with the enzyme. Column 5 (“formed from ¹²CH₄”) lists all products derived from ¹²CH₄ (natural abundance) introduced into the headspace. ^bEstimated relative errors of integration are 2% for the assay solution and 5% for the headspace gas. ^cFrom natural abundance of ²H (determined to be 131 ppm in the ¹²CH₄ used) and ¹³C (1.1%). ^dThe small amount of ¹²CH₂D-S-CoM measured is mainly (4 nmol) due to ²H incorporation into the unlabeled starting material (= 1% of the 411 nmol ¹³CH₂D-S-CoM formed). ^e21 nmol arises from the 1% unlabeled ¹²CH₃-S-CoM present in the initial substrate.

Further, the ¹²CH₄ consumed is converted to ¹²CH₃-S-CoM exclusively (320 nmol, 21 turnovers per enzyme), showing that no deuterium incorporation occurs during the process of methane activation. The selective formation of nondeuterated

methyl-coenzyme M rules out pathways B and C at the same time (deuterium incorporation into the intermediate and isotope exchange in the substrate formed).

Note that the reaction along pathway C (described as the first result in this contribution) does proceed to give ¹³CH₂D-S-CoM in the first ~25 s, until practically all coenzyme B is used up. Once equilibrium is established (~0.5–32 min) the concentration of coenzyme B is very low (est. ~0.5 μM), the forward and reverse reactions occur at the same low rate, and deuterium exchange into the substrate is no longer detectable.

In summary, the CH₄ activated is transformed to CH₃-S-CoM exclusively, even though D₂O buffer is used as the solvent.

This result has two important consequences. First, it demonstrates that the active site of the enzyme is shielded, which means that, once both substrates are bound (or both products), there is no isotope exchange with the solvent. The hydrogen (or deuterium) atoms involved in the reaction are carried into the active site only via the thiol group of coenzyme B, or in the reverse reaction, via methane. Second, the absence of H/D exchange from the medium into the ternary complexes makes it possible to study isotope effects for methane activation, because the methyl-coenzyme M formed from methane does not undergo isotope exchange and can therefore be analyzed in order to determine the isotope effect.

Isotope Effect on Methane Activation in Experiments with Intermolecular Competition. Activation of a mixture of CH₄ and CD₄ is performed under the conditions described above. The amount of CH₃-S-CoM and CD₃-S-CoM formed is determined via ¹H and ²H NMR spectroscopy (Table 4). Statistical analysis of the three experiments results in an isotope effect for CH₄ activation vs CD₄ activation of 3.9 ± 0.6.

Isotope Effect on Methane Activation in Experiments with Intramolecular Competition. When methane activation is carried out with CH₂D₂ as the substrate, the isotope effect can be determined directly from the ratio of CHD₂-S-CoM/CH₂D-S-CoM formed. Experiments are performed in deuterated and undeuterated buffer (Table 5). Statistical evaluation of all five experiments results in a kinetic isotope effect of 2.09 ± 0.15.

Calculation of Primary and Secondary Kinetic Isotope Effects on Methane Activation. Assuming that the degree of deuteration has no significant effect on methane binding, the primary and the secondary isotope effects on methane activation can be calculated if they act on the same transition state. The isotope effect on CH₄/CD₄ activation equals a primary combined with a triple secondary kinetic isotope effect; the isotope effect of C–H vs C–D activation in CH₂D₂ equals a primary divided by a secondary kinetic isotope effect.

Table 4. Isotope Effect on Methane Activation from a Mixture of CH₄ and CD₄ Determined from the Relative Amount of CH₃-S-CoM and CD₃-S-CoM Formed^a

experiment	Me-S-CoM total [μmol]	¹² CH ₃ -S-CoM formed ^b [μmol]	¹² CD ₃ -S-CoM formed [μmol]	ratio ¹² CH ₃ -/ ¹² CD ₃ -S-CoM formed	KIE corr. ^c
H ₂ O, Run 1	2.96	0.414	0.099	4.17	3.61
H ₂ O, Run 2	2.92	0.451	0.100	4.51	3.91
D ₂ O	3.03	0.466	0.100	4.68	4.05

^aBoth H₂O and D₂O buffers are used as the solvent and do not show significant differences. ^bCorrected for the small amount of ¹²CH₃-S-CoM present in the starting material (99% ¹³C). ^cThe ratio ¹²CH₃-S-CoM/¹²CD₃-S-CoM formed was corrected for the ratio CH₄/CD₄ measured in the gas mixture employed (53.57%/46.43%)

Table 5. Activation of CH₂D₂ in H₂O and D₂O Buffer

experiment	Me-S-CoM [μmol]	CH ₂ D ₂ activated [μmol]	KIE = CHD ₂ -S-CoM formed per CH ₂ D-S-CoM formed
H ₂ O, run 1	2.656	0.892	2.160
H ₂ O, run 2	2.681	0.791	2.233
D ₂ O, run 1	2.862	0.678	2.038
D ₂ O, run 2	2.967	0.384	1.922
D ₂ O, run 3 ^a	2.560	0.290	2.091

^aFor this experiment, twice the amount of enzyme but only 0.2 bar CH₂D₂ was used.

The following values are obtained (see S1.8 in the SI for detailed calculation):

$$\text{primary kinetic IE: } k_{\text{H}}/k_{\text{D}} = 2.44 \pm 0.22$$

$$\text{secondary kinetic IE: } k_{\text{H}}/k_{\text{D}} = 1.17 \pm 0.05$$

DISCUSSION

The first step (transition state “TS 1”, or “TS 1a and TS 1b”, Figure 4) leading from the substrates ternary complex to the

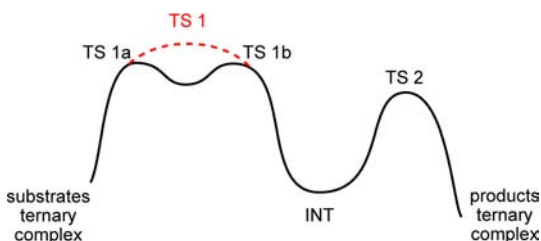


Figure 4. Schematic reaction profile taking into account the intermediate discovered previously.

intermediate (“INT”) is rate-limiting because formation of methane is 25 times faster than the reaction back to the substrates.

The presence of a substantial carbon isotope effect (1.04 ± 0.01) proves that either cleavage of the C–S bond in the substrate, formation of the C–H bond, or both occur in the rate-limiting step (TS 1). We interpret the carbon isotope effect as being mainly due to the breaking of the C–S bond because a larger H/D primary kinetic IE than the one observed ($k_{\text{H}_2\text{O}}/k_{\text{D}_2\text{O}} = 1.3 \pm 0.3$) would be expected if formation of the C–H bond were the main contributor to the ¹²C/¹³C-IE.

The isotope exchange experiments described previously show that all four C–H bonds of methane are already present in the intermediate.²² Whether this state corresponds to methane prevented from leaving the active site for steric reasons or to methane bound to nickel as a σ -complex cannot be decided, because the second transition state (TS 2) is lower in energy and thus cannot be probed for by kinetic isotope effects. In the reverse reaction, the activation of methane, kinetic isotope effects are also due to TS 1 (microscopic reversibility), but TS 2 might contribute via equilibrium isotope effects.

The experiment of methane activation in deuterated medium showed formation of CH₃-S-CoM exclusively. It follows that the intermediate cannot exchange deuterium with the solvent. Accordingly, in the methane-forming direction, the rate-limiting step defines the isotopic composition of the methane moiety in the intermediate.

In the following discussion of mechanisms that are compatible with the observed isotope effects, two different scenarios concerning the nature of the step(s) leading to the intermediate will be considered:

- A concerted reaction where C–S bond breaking and C–H bond making occur in a single step (TS 1, drawn red in Figure 4).
- Stepwise methane formation where TS 1a corresponds to the cleavage of the C–S bond, followed by formation of the C–H bond as a distinct but not rate-limiting step, TS 1b (black curve in Figure 4).

Methane Formation by Concerted C–S Breaking and C–H Formation (A). On the basis of DFT calculations, Siegbahn and co-workers proposed a mechanism in which C–S bond breaking and C–H bond formation occur in a single step, although not synchronously.^{13,30,31} In this mechanism the Ni(I) center attacks the sulfur of Me-S-CoM (and not the methyl group) according to a radical substitution leading to a Ni(II) thiolate and releasing a methyl radical, which concurrently abstracts a hydrogen atom from the SH group of CoB-SH. In the calculated transition state (Figure 5) the C–S bond is broken to a large extent, whereas the nascent C–H bond is still extremely long. In other words, this transition state contains an almost free methyl radical.³⁰

A quantitative comparison of our experimental isotope effects with those predicted by the DFT calculation has to await

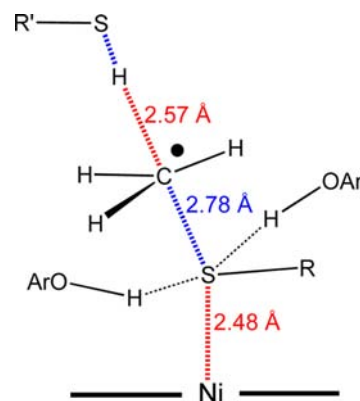


Figure 5. TS 1 according to Siegbahn and co-workers.³⁰ Two bonds are broken (C–S and S–H, drawn blue) and two bonds are formed (Ni–S and C–H, drawn red) in a single step. Coenzyme F430 is depicted as “Ni”, R mimics CoM, and R’ mimics CoB. OAr depicts phenol groups used as a model for the tyrosine residues.

extension of the calculations to include isotope effects, which is under way in the laboratory of the authors of the DFT study.³² Qualitatively, the presence of a nearly free methyl radical in TS 1 suggests comparing the experimental kinetic IEs with those reported for the formation of methyl radicals by homolysis. We could not find data for the isotope effects on formation of methyl radicals by homolysis of a C–S bond in the literature. For the homolytic C–C cleavage of dimethylphenylcarbinyl alkoxy radical to give a methyl radical and acetophenone, secondary isotope effects of 1.17 (–9 °C) and 1.12 (75 °C) per D have been reported.^{33,34} These values are very similar to those reported here for methane formation (1.19 per D) and methane activation (1.17 per D), consistent with a change of hybridization from sp³ to sp² upon going to the transition state.

The absence of a significant primary isotope effect on CH₄ vs CH₃D formation (1.3 ± 0.3, see Introduction) is in line with this mechanism, because the interaction of the carbon with the incoming hydrogen is very weak in the calculated transition state (long nascent bond). For the bimolecular reaction of •CH₃ radicals with a thiol in solution, a primary isotope effect of 2.71 has been reported.³⁵ Since this value applies to a bimolecular reaction in solution at unrestrained collision geometries, we consider it as an upper limit for the MCR case.

Multistep Reactions for Methane Formation (B). If the mechanism discussed above were to involve a free methyl radical as a true intermediate (two steps to the intermediate, as originally proposed in Siegbahn's first paper¹³), rotation of •CH₃ would lead to a loss of stereospecificity, inconsistent with the finding that the homologous substrate ethyl-coenzyme M gives ethane under net inversion of configuration.²¹ Hence, only a "transient alkyl radical", already interacting with the S–H group of coenzyme B, can explain conservation of stereospecificity.

A sequence leading from the substrate ternary complex to the intermediate in more than one step is required for mechanisms involving initial attack of the nickel center at the methyl group or the C–S bond of Me-S-CoM (TS 1a). Transfer of hydrogen to form the intermediate containing methane is then required as a second, separate step (TS 1b).

A mechanism of this type was proposed a long time ago. It involves nucleophilic attack of the Ni(I) center at the carbon atom of Me-S-CoM in S_N2 fashion to yield a methyl-Ni(III) species.^{17,18,36,37} This S_N2 reaction accounts for the inversion of configuration, provided that methane formation from the Me-Ni(III) intermediate occurs under retention.

The putative methyl-Ni(III) intermediate has been generated independently by adding methyl halides to the active Ni(I) enzyme and is characterized by EPR spectroscopy.^{38,39} However, the formation of a methyl-Ni(III) species upon treatment of the active enzyme with methyl halides has no evidentiary value without proof that it can also be formed from Me-S-CoM. Additionally, secondary isotope effects for S_N2 reactions are typically small or even inverse, although larger values have been found for very loose transition states.⁴⁰ Oxidative additions of MeI to organoplatinum(II) complexes showed α -secondary kinetic IEs up to 1.04/D,⁴¹ distinctly smaller than the secondary kinetic IE of 1.19/D we measured. The reaction of free Ni(I)F430 pentamethyl ester with trialkylsulfonium ions giving methane follows the selectivity pattern expected for an S_N2 reaction (methyl ≫ isopropyl > *tert*-butyl).^{42,43} We have determined the intermolecularly competitive α -secondary kinetic IE in the corresponding reaction with (CH₃)(CD₃)₂S⁺ to be 1.06/D (see S1.5 in SI),

similar to that found for oxidative addition in ref 41 but distinctly smaller than that for the MCR reaction with methyl-coenzyme M.

Other conceivable mechanisms, such as an initial oxidative addition of the C–S bond to the Ni(I) center, yielding a methyl-thiolato-Ni(III) species or an initial formation of a Ni(III)hydride (which then reacts with CH₃-S-CoM in the rate-determining step to give methane and presumably, a Ni(III)-thiolato complex) are difficult to judge in the light of our experimental isotope effects because, to our knowledge, there are no chemical precedents.

Methane Activation in One Step Yielding Methyl-Coenzyme M (A). The primary kinetic H/D isotope effect for methane formation is small (1.3 ± 0.3, see Introduction), but for the reverse reaction, the kinetic IE ($k_{\text{H}}/k_{\text{D}} = 2.44$) is significant. If these values correspond to intrinsic isotope effects of a single rate-limiting step without attenuation through equilibrium isotope effects in preceding, non-rate-limiting steps, the ratio of forward and reverse primary kinetic IEs should correspond to the equilibrium IE of the overall reaction catalyzed by MCR. The main contribution to this equilibrium isotope effect is expected to stem from different fractionation factors ($\Phi = K_{\text{D}}/K_{\text{H}}$) of a C–H bond in methane and the S–H bond in CoB-SH. Fractionation factors for C(sp³)–H bonds are close to $\Phi = 1.0$, whereas for thiol S–H bonds they are typically 0.4–0.5 (0.42 was determined experimentally for CoB-SH, see our forthcoming publication on solvent isotope effects). This estimate would predict an equilibrium IE of $K_{\text{H}}/K_{\text{D}} = 0.42$, which is within the range of our best estimate for the ratio of the kinetic isotope effects $\text{IE}_{\text{fwd}}/\text{IE}_{\text{rev}}$ of $(1.3 \pm 0.3)/2.44 = 0.41\text{--}0.53$.

The mechanism proposed by Siegbahn and co-workers requires that, in the methane activating direction, a thiyl radical abstracts a hydrogen atom from methane. This very endothermic reaction ($\Delta H^\circ = \sim 70 \text{ kJ mol}^{-1}$) is not observed in nonenzymatic reactions because other follow-up reactions of thiyl radicals such as dimerization are much faster in solution. Hence, no experimental isotope effects are reported, and comparison with our values would have to rely on quantum mechanical calculations. Since the active site of MCR contains no easily abstractable hydrogens, with the exception of the two phenolic tyrosine OH groups, a thiyl radical might persist for the time needed to react with methane, unlike that in solution.

The secondary isotope effect on methane activation (1.17) is also compatible for methyl radical formation from methane (respectively, a methyl radical-like transition state), since the fractionation factor Φ for the H–CH₃ moiety in methane is expected to be similar to that for the H–CH₂S group.

Organometallic Methane Activation in a Multistep Reaction (B).⁴⁴ Isotope exchange experiments prove that an intermediate with all four C–H bonds of methane must be formed in the methane-forming direction.²² This intermediate contains either methane held in the active site by noncovalent interactions or, alternatively, methane bound to the metal, i.e. as a σ -complex. Coordination of a C–H bond to Ni in the intermediate would weaken this bond in the methane-activating direction for cleavage according to one of the established mechanisms observed in organometallic C–H activation such as oxidative addition/reductive elimination, electrophilic activation, or σ metathesis. The isotope effect of $k_{\text{H}}/k_{\text{D}} = 2.44$ reported here matches known isotope effects for oxidative cleavage. Periana and Bergmann reported a primary isotope effect of 2.5 for the reaction of coordinated ethane to yield a

hydrido ethyl rhodium complex.⁴⁵ As pointed out by Jones,⁴⁶ net isotope effects observed for oxidative addition/reductive elimination are typically equilibrium isotope effects corresponding to the ratio of the kinetic isotope effects for oxidative cleavage and reductive coupling, respectively.

If methane activation by MCR were to involve oxidative addition, this step would precede the rate-limiting step (C–S bond-breaking/formation) and manifest itself only as an equilibrium isotope effect modulating the overall observable kinetic IE. In the methane-forming direction, however, any isotope effects on the corresponding reductive elimination after the rate-limiting step would be masked, and the observed IE would correspond to the intrinsic IE for the rate-limiting step.

Electrophilic activation of methane by reactive platinum IV species typically exhibits larger primary kinetic IEs ($k_{\text{H}}/k_{\text{D}} \approx 6\text{--}7$) than the one observed here.^{47,48} In cases where C–H bond activation has been interpreted in terms of a σ -bond metathesis mechanism, the intrinsic kinetic IE of the σ -bond metathesis step has been found to be $k_{\text{H}}/k_{\text{D}} = 2.65$, quite close to the value reported here.^{49,50} Since this step is generally preceded by a rate-limiting coordination of the (aromatic) hydrocarbon, however, its intrinsic kinetic IE is only observable via product distribution in intramolecular competition experiments. In the case of methane activation by MCR considered here, the rate-limiting step occurs after any potential σ -bond metathesis step, and at most, the equilibrium IE of the latter would modulate the observed overall IE. The difference between the kinetic IEs for intermolecular (2.09) and intramolecular (3.9) competition (CD_4/CH_4 vs CH_2D_2) found here can be explained from statistical factors and α -secondary isotope effects of the same order of magnitude as found for the methane-forming direction and does not require the presence of an additional equilibrium IE in a preceding equilibrium.

Implications of a Putative Coupling between the Two Active Sites. The presence of two active sites in the enzyme provoked the thought that they might cooperate in order to perform the catalytic reaction in what has been termed a “two stroke engine” mode.⁵¹ If the enzyme couples an endergonic step at one active site with an exergonic step at the other active site, isotope effects for steps that would not be rate-limiting in a single uncoupled active site might manifest themselves in the observed overall kinetic IE of a coupled reaction of both active sites. On the other hand, intrinsic isotope effects could be masked or diminished by a coupling of the two active sites. So far, experimental results on MCR, including the isotope effects reported here, have not provided hard evidence for a mechanistic coupling of the two active sites. Certain facts and observations do, however, suggest that such a coupling might exist and should be investigated in detail in further experiments: First, the MCR_{red2} enzyme states observed when coenzyme B and coenzyme M are added to the active enzyme can only be induced to a maximal 50% of the total spin.⁵² Second, UV–vis spectra (see S1.7 in SI) show that, under the equilibrium conditions we used to study methane activation, exactly half of the active sites have been transformed from Ni(I) (MCR_{red1}) to a species with a UV–vis spectrum resembling that of the Ni(II) form or a X–Ni(III) form (the X–Ni(III) enzyme states MCR_{ox1} and MCR_{Me} are known to show absorption bands similar to Ni(II) forms^{53,54}).

Although 52 Å apart from each other, the two active sites are connected by the α and α' protein chains that are both part of both active sites. The α -chains contain the unprecedented thioglycine residues $\alpha 445$ ($\alpha' 445$), which, since they are

conserved in the MCR sequences of all methanogens and probably also of all ANME organisms investigated,⁵ point to a crucial mechanistic function. In the X-ray structure of the inactive $\text{MCR}_{\text{ox1-silent}}$ state,¹⁷ the sulfur of thioglycine $\alpha 445$ is ~ 6 Å distant from the SH group of coenzyme B. One might therefore speculate that its role is to interact with coenzyme B (or a coenzyme B-derived thyl radical) and thus provide conformational coupling to the other active site via the α -chain in a particular intermediate state of the catalytic cycle.

CONCLUSIONS

This study shows that the ternary complexes of MCR, $\text{CH}_3\text{-S-CoM}$, and coenzyme B are shielded from hydrogen exchange with the medium. The isotope effects reported here indicate that breaking of the carbon–sulfur bond is rate limiting and that the CH_3 group of the substrate changes its geometry from tetrahedral to trigonal planar upon going to the transition state of this step. The α -secondary kinetic IE is distinctly larger than expected for an $\text{S}_{\text{N}}2$ -type attack of Ni(I) on the methyl group proposed in an earlier mechanistic hypothesis.^{17,18,36,37} On the other hand, these findings are compatible with qualitative expectations for the radical substitution mechanism proposed by Siegbahn and collaborators in which C–S bond breaking and C–H bond formation occur in a single step.³⁰ Because there are no precedent cases in the literature, the question, whether the small primary H/D kinetic IE in the methane-forming direction and the significant primary kinetic IE in the methane-activating direction would also be in line with this mechanism has to await the results of quantum chemical (or preferably QM/MM) calculations. The primary kinetic H/D IE for methane activation is also close to the values reported for equilibrium isotope effects in oxidative cleavage/reductive coupling or σ -bond metathesis reactions, which, in the case of MCR, would also be equilibrium isotope effects for steps preceding the rate-limiting one. Therefore, this type of mechanism is also reasonable in light of our results. Our current interpretation is based on the assumption that the catalytic cycles at the two active sites operate independently. However, indirect evidence points to the possibility that they are coupled. Clearly, further investigation of such coupling is indicated and might shed light on the role of the unique and conserved thioglycine residue in MCR.

EXPERIMENTAL PROCEDURES

Assay Conditions. Two different types of assays were used, depending on the purpose of the experiment. (I) Assays were limited in the second substrate coenzyme B. In this case, equilibrium was attained when practically all CoB was used up, and both $\text{CH}_3\text{-S-CoM}$ and CoM-S-S-CoB were present. (II) Assays were not limited by the second substrate due to continuous reduction of the formed CoM-S-S-CoB with Ti(III)-citrate regenerating CoB-SH.

For coenzyme B-limited assays (type I), the first substrate (methyl-coenzyme M) is in excess, and 0.2 or 0.5 equiv of the second substrate (coenzyme B) is added. The concentration of the product methane stays low due to diffusion (or bubbling) out of the solution into the headspace. The second product heterodisulfide accumulates. Because methane formation and deuterium incorporation into the substrate cease after coenzyme B is consumed, the conversion can be controlled to reach a maximum of 20% or 50% maximal conversion. The enzyme state after conversion of the coenzyme B to the heterodisulfide allows methane activation to occur. We used methane with natural abundance of ^{13}C in the headspace and $^{13}\text{CH}_3\text{-S-CoM}$ as the substrate, which allowed quantification of methane activation by analyzing the amount of newly formed ^{12}C -substrate.

For experiments designed to achieve high conversions to methane, the reductant Ti(III)-citrate was added in excess (assay type II). Ti(III)-citrate converts the product heterodisulfide into the weaker inhibitor coenzyme M and regenerates the second substrate coenzyme B simultaneously. This reaction is catalyzed by 0.3 mM hydroxycobalamin added to the assays.

For each set of experiments, a stock solution containing 50 mM potassium phosphate buffer, pH = 7.6 in H₂O or D₂O, both substrates, and Ti(III)-citrate (for assays type II) was prepared under ice cooling without enzyme. One aliquot was removed as a reference ("0 min value" or control). The remaining amount was supplemented with enzyme and distributed to different vials (1.60 mL each). The assay volume (liquid phase) was 1.60 mL for all experiments. After sealing with a rubber stopper, the vials were immediately incubated at 60 °C in a water bath shaker. For assays without Ti(III)-citrate the reaction was stopped after the desired reaction time by addition of 1 mL air with a syringe. The assays containing Ti(III)-citrate were stopped by injection of 50 μL HClO₄, 70% (or DClO₄, 68% in D₂O).

All substrates and products involved in the reaction were analyzed via NMR spectroscopy in order to deduce fractions of conversion (heterodisulfide) and the isotopic composition in the remaining substrate and in the methane formed.

NMR Measurements. ¹H NMR spectra were recorded on a Bruker Avance II 600 MHz spectrometer with an inverse detection probe. ²H NMR spectra were recorded on a Bruker Avance III 600 MHz spectrometer with a cryodetection probe.

The assay solutions were centrifuged, and 620 μL was transferred into an NMR tube. After addition of 80 μL dioxane solution (0.025% v/v dioxane and 0.025% v/v dioxane-*d*₈ in D₂O) as an internal standard, the spectra were recorded at 298 K without spinning (30° excitation pulse, 5 s acquisition time). CW-presaturation of the water signal for 2 s was employed for the assays in H₂O and 2 s relaxation delay for the samples in D₂O to ensure a uniform repetition rate of 7 s for all samples.

Methane was passed through CDCl₃ with a fine needle to absorb the methane and measured with a 5 s relaxation delay (10 s repetition rate).

Assays with deuterium-containing isotopologues were acquired with and without broadband deuterium decoupling, denoted ¹H{²H}.

The integration was carried out with the software BRUKER Topspin 2.1 relative to the internal standard dioxane (set to 3.70 ppm for ¹H and for ²H measurements).

Fitting of NMR spectra was carried out with the software iNMR 4.1.7 for the determination of the enrichment in the ¹³C label for assays in which the ¹²C/¹³C kinetic isotope effect was measured.

The fraction of conversion was determined by comparing the amount of disulfides formed with the amount of remaining substrate, using the integrals of the CH₂ group R-(S)-S-CH₂CH₂SO₃⁻ (for Me-S-CoM, CoB-S-S-CoM, and CoM-S-S-CoM).

Measurement of Isotope Effects on Methane Formation. For the experiment aiming to measure the ratio of methane formation vs deuterium incorporation, 4 mM methyl-coenzyme M and 2 mM coenzyme B were used to limit the maximal conversion to about 50% (after which deuterium incorporation also stops).

Because the reaction is slower at lower temperatures, more enzyme was used as follows: 1.1 nmol (0.69 μM) for 60 °C, 2.1 nmol (1.31 μM) for 40 °C, 8.6 nmol (4.25 μM) for 22 °C, and 21.4 nmol (13.4 μM) for 4 °C. The assays were incubated for 4 min at the different temperatures and analyzed via ¹H NMR spectroscopy. The fraction of deuterium incorporation was determined from the integral values of the spectra acquired with deuterium decoupling.

Deuterium incorporation into methyl-coenzyme M is dependent on the second substrate coenzyme B. Once coenzyme B is consumed, methane formation and deuterium incorporation into the substrate halts as confirmed via separate experiments.

Carbon Isotope Effect on Methane Formation. The assay solution contained 5 mM CH₃-S-CoM with natural isotopic composition, 5 mM ¹³CH₃-S-CoM, 0.5 mM coenzyme B homodisulfide, 0.3 mM hydroxycobalamin and 25 mM Ti(III)-citrate in 50 mM potassium phosphate buffer pH = 7.6.

Enzyme, 1.3 nmol, 0.81 μM, per assay was added. After incubation of the vials at 60 °C for 2, 3, 4, 5, 5.5, and 6 min, the reaction was stopped by injection of 50 μL HClO₄ (70%). The centrifuged assay solutions were analyzed via ¹H NMR spectroscopy in order to determine the fraction of conversion and ratios of ¹²CH₃-S-CoM vs ¹³CH₃-S-CoM in each assay. The method of measuring heavy-atom isotope effects via ¹H NMR spectroscopy had been validated previously.⁵⁵ The enrichment in the ¹³C-label was determined by fitting the NMR spectra with the program iNMR (see S2.2 in SI for overlays of the fitted and measured spectra). Calculation of the isotope effect for each time point is listed in the SI (Table S1.3).

Stopping the reaction via addition of HClO₄ in the presence of an excess Ti(III)-citrate converted some of the remaining methyl-coenzyme M to the corresponding sulfoxide. The fraction of sulfoxide formed was taken into account for the calculation of the fraction of conversion (see S1.2 in the SI for details). The enrichment in the ¹³C label, however, was always determined via analysis of the signals due to unoxidized Me-S-CoM.

Secondary Isotope Effect on Methane Formation. The assay solution contained 5 mM ¹³CH₃-S-CoM, 5 mM CD₃-S-CoM, and 2 mM coenzyme B in 50 mM potassium phosphate buffer pH = 7.6.

Incubation with 1.1 nmol enzyme per assay (0.69 μM) at 60 °C for 4 min yielded about 20% conversion (consumption of all the coenzyme B) to methane, which was analyzed via ¹H{²H} NMR spectroscopy.

The ratio in of the two isotopologues in the substrate was measured by ¹H- and ²H NMR spectroscopy relative to the internal standard acetonitrile (1:1 mixture of acetonitrile and acetonitrile-*d*₃). A ratio of ¹³CH₃-S-CoM/CD₃-S-CoM = 44.2%/55.8% was measured and the isotope effect corrected for this value (see S1.3 in the SI).

The measurement of the secondary isotope effect on methane formation in assays containing Ti(III)-citrate is described in S1.4 in the SI.

Methane Activation in Deuterated Medium, Shielding of the Active Site. Assays were prepared with 4 mM ¹³CH₃-S-CoM and 2 mM coenzyme B. After addition of enzyme (15 nmol per assay, 9.4 μM) and sealing with a rubber stopper, the headspace gas (N₂/H₂) was replaced by methane at atmospheric pressure (5 mL, 200 μmol), with the use of a gas manifold inside the anaerobic tent.

Already during warming up to 60 °C, the second substrate CoB-SH reacted quickly with half of the substrate ¹³CH₃-S-CoM to the concentrations shown in Table 6.

Table 6. Concentrations in the Equilibrium State where Methane Activation Proceeds

substrate or product	concentration in solution [mM]	total amount [μmol]
¹³ CH ₃ -S-CoM	~2	3.2
CoB-SH	~0	~0
CoB-S-S-CoM	~2	3.2
¹² CH ₄	~1 ^a	200

^aSolubility of methane at 60 °C [extrapolated from ref S6].

Under these conditions, in which both heterodisulfide (CoB-S-S-CoM) and methane were present, methane activation occurred and could be detected by the formation of ¹²CH₃-S-CoM.

For the methane employed, a natural abundance of 1.1% for ¹³C was assumed. The ²H-content was determined to be 131 ppm (524 ppm CH₃D) by NMR.

Isotope Effect on Methane Activation (Intermolecular Competition). A gas cylinder (500 mL) was evacuated (<0.01 mbar), charged with CD₄ (99% deuterium, Cambridge Isotope Laboratories) to one bar overpressure (2 bar CD₄). Next, CH₄ (natural isotopic composition) was added to 3 bar total pressure (2 bar CH₄). The exact ratio of isotopologues was measured by passing the gas through CDCl₃ containing an internal standard (acetonitrile/acetonitrile-*d*₃ (1:1)). The solution was allowed to equilibrate with the headspace of the NMR tube for about one hour. ¹H NMR spectra and

^2H NMR spectra (with presaturation of the CDCl_3 signal) were carried out, giving a ratio of $\text{CH}_4/\text{CD}_4 = 53.57\%/46.43\%$. The influence of the presaturation ($^{12}\text{CDCl}_3$ signal) on the integral ratio was negligible since both of the $^{13}\text{CDCl}_3$ satellites remained without significant change. The diffusion of methane out of the sample tube was judged to be negligible, because ^3H NMR spectra and ^2H NMR spectra were recorded alternately and did not show significant changes.

All corresponding experiments were performed with 1 bar methane from this gas mixture by using the gas manifold inside the anaerobic tent. The assays contained 4 mM $^{13}\text{CH}_3\text{-S-CoM}$ and 2 mM coenzyme B and 10.7 nmol enzyme per assay (6.69 μM). The incubation time was 30 min at 60 °C.

The analysis was carried out via ^1H - and ^2H NMR spectroscopy, applying H_2O or D_2O presaturation where required. Integration was performed relative to the identical mixture of acetonitrile and acetonitrile- d_3 used for the analysis of the methane employed.

Isotope Effect on Methane Activation (Intramolecular Competition). CH_2D_2 (98%, Cambridge Isotope Laboratories) was introduced into an evacuated 100-mL serum bottle (0.5 bar overpressure), which contained freshly activated $\text{Cu}/\text{Al}_2\text{O}_3$ catalyst (for drybox use), in order to remove the traces of oxygen that were present in the delivered product. ($^1\text{H}\{^2\text{H}\}$ NMR analysis showed the presence of 3.70 mol % CH_3D in the gas purchased, which was neglected for the evaluation of the isotope effect.)

The assays contained 4 mM $^{13}\text{CH}_3\text{-S-CoM}$, 2 mM coenzyme B, and 22 nmol enzyme (13.8 μM) per assay. The headspace was evacuated inside the anaerobic tent and 5 mL CH_2D_2 injected via a syringe (corresponding to 1 bar absolute pressure). Incubation time: 15 min.

The analysis was carried out via $^1\text{H}\{^2\text{H}\}$ NMR spectroscopy by comparing the amount of $\text{CH}_2\text{D-S-CoM}$ formed with the amount of $\text{CHD}_2\text{-S-CoM}$ formed.

Purification of MCR. Growth of archaea, purification of the enzyme, and all assay preparations (including exchange of the headspace gas by methane) were carried out strictly anaerobically in a tent (Coy instruments), filled with N_2/H_2 (95%/5%) that was equipped with a Pd-catalyst. All buffers used were boiled while gassed with a stream of N_2 , cooled under vacuum, and brought into the anaerobic tent after applying an overpressure of N_2 . Before use, the buffers were stirred overnight in the anaerobic tent with the lid of the bottle off.

Methanothermobacter marburgensis was grown under H_2/CO_2 (80%/20%) in 10-L cultures at 65 °C to an optical density of 5–6 at 578 nm, as described previously.⁵⁷ Methyl-coenzyme M reductase isoenzyme I was purified in the active Ni(I) valence form (>90% Ni(I), see Figure S1.1 in SI for the UV-vis spectrum) and separated from the other isoenzyme.²⁰ For a recent review about the purification details see ref 58. The concentration of the enzyme solution (~1 mL; ~0.7–1 mM, corresponding to 20–28% by weight) was determined by UV-vis spectroscopy after oxidation of an aliquot enzyme with air to the Ni(II) form ($\epsilon_{420} = 44,000 \text{ l mol}^{-1} \text{ cm}^{-1}$). The quantities of enzyme indicated for each experiment are not corrected for the small amount of inactive enzyme (always $\leq 10\%$).

Synthesis of Substrates. Labeled and unlabeled substrates were synthesized as described previously.^{9,22,59} For Me-S-CoM, the sodium salt was used, for CoB-SH the diammonium salt, and for CoB-S-S-CoB the tetraammonium salt. All substrates were >98% pure according to NMR.

$^{13}\text{CH}_3\text{-S-CoM}$ was prepared from $^{13}\text{CH}_3\text{I}$ (99% ^{13}C , Cambridge Isotope Laboratories). Scale: 4.45 g, 31.1 mmol; yield: 3.3 g, 18.4 mmol, 61%.

$\text{CD}_3\text{-S-CoM}$ was prepared from CD_3I (>99% D, Dr. Glaser AG). Scale: 1.5 g, 10.3 mmol; yield: 1.272 g, 7.02 mmol, 70%.

■ ASSOCIATED CONTENT

Ⓢ Supporting Information

Additional figures, details of experimental procedures, and acquired and measured NMR spectra. This material is available free of charge via the Internet at <http://pubs.acs.org>.

■ AUTHOR INFORMATION

Corresponding Author

jaun@org.chem.ethz.ch

Present Address

[§]Division of Geological and Planetary Sciences, California Institute of Technology, 1200 E. California Blvd., Pasadena, CA 91125, United States.

Notes

The authors declare no competing financial interests.

■ ACKNOWLEDGMENTS

This work was supported by the Swiss National Science Foundation (S.S. and B.J.; Grant 200020-134476) and the Max Planck Society and the Fonds der Chemischen Industrie (M.G. and R.K.T.). We thank Reinhard Böcher for technical assistance.

■ REFERENCES

- (1) Jaun, B.; Thauer, R. K. *Met. Ions Life Sci.* **2007**, *2*, 323–356.
- (2) Knittel, K.; Boetius, A. *Annu. Rev. Microbiol.* **2009**, *63*, 311–334.
- (3) Mayr, S.; Latkoczy, C.; Kruger, M.; Gunther, D.; Shima, S.; Thauer, R. K.; Widdel, F.; Jaun, B. *J. Am. Chem. Soc.* **2008**, *130*, 10758–10767.
- (4) Krueger, M.; Meyerdierks, A.; Gloeckner, F. O.; Amann, R.; Widdel, F.; Kube, M.; Reinhardt, R.; Kahnt, J.; Boecher, R.; Thauer, R. K.; Shima, S. *Nature* **2003**, *426*, 878–881.
- (5) Shima, S.; Krueger, M.; Weinert, T.; Demmer, U.; Kahnt, J.; Thauer, R. K.; Ermler, U. *Nature* **2012**, *481*, 98–101.
- (6) Boetius, A.; Ravensschlag, K.; Schubert, C. J.; Rickert, D.; Widdel, F.; Gieseke, A.; Amann, R.; Jorgensen, B. B.; Witte, U.; Pfannkuche, O. *Nature* **2000**, *407*, 623–626.
- (7) Hinrichs, K. U.; Hayes, J. M.; Sylva Sean, P.; Brewer, P. G.; DeLong Edward, F. *Nature* **1999**, *398*, 802–805.
- (8) Hallam, S. J.; Putnam, N.; Preston, C. M.; Detter, J. C.; Rokhsar, D.; Richardson, P. M.; DeLong, E. F. *Science* **2004**, *305*, 1457–1462.
- (9) Scheller, S.; Goenrich, M.; Boecher, R.; Thauer, R. K.; Jaun, B. *Nature* **2010**, *465*, 606–608.
- (10) Dey, M.; Li, X.; Zhou, Y.; Ragsdale, S. W. In *Organometallics in Environment and Toxicology*; Sigel, A., Sigel, H., Sigel, R. K. O., Eds.; Metal Ions in Life Sciences, Vol. 7; RSC Publishing: Cambridge, U.K., 2010; pp 71–110.
- (11) Duin, E. C.; McKee, M. L. *J. Phys. Chem. B* **2008**, *112*, 2466–2482.
- (12) Ermler, U.; Grabarse, W.; Shima, S.; Goubeaud, M.; Thauer, R. K. *BIOspektrum* **1998**, *4*, 20–24.
- (13) Pelmentschikov, V.; Blomberg, M. R. A.; Siegbahn, P. E. M.; Crabtree, R. H. *J. Am. Chem. Soc.* **2002**, *124*, 4039–4049.
- (14) Goubeau, M.; Schreiner, G.; Thauer, R. K. *Eur. J. Biochem.* **1997**, *243*, 110–114.
- (15) Jaun, B.; Pfaltz, A. *J. Chem. Soc., Chem. Commun.* **1986**, 1327–1329.
- (16) Rospert, S.; Boecher, R.; Albracht, S. P. J.; Thauer, R. K. *FEBS Lett.* **1991**, *291*, 371–375.
- (17) Ermler, U.; Grabarse, W.; Shima, S.; Goubeaud, M.; Thauer, R. K. *Science* **1997**, *278*, 1457–1462.
- (18) Goenrich, M.; Mahlert, F.; Duin, E. C.; Bauer, C.; Jaun, B.; Thauer, R. K. *J. Biol. Inorg. Chem.* **2004**, *9*, 691–705.
- (19) Gunsalus, R. P.; Romesser, J. A.; Wolfe, R. S. *Biochemistry* **1978**, *17*, 2374–2377.
- (20) Bonacker, L. G.; Baudner, S.; Moerschel, E.; Boecher, R.; Thauer, R. K. *Eur. J. Biochem.* **1993**, *217*, 587–595.
- (21) Ahn, Y.; Krzycki, J. A.; Floss, H. G. *J. Am. Chem. Soc.* **1991**, *113*, 4700–4701.
- (22) Scheller, S.; Goenrich, M.; Mayr, S.; Thauer, R. K.; Jaun, B. *Angew. Chem., Int. Ed.* **2010**, *49*, 8289–8292.
- (23) Pine, M. J.; Barker, H. A. *J. Bacteriol.* **1956**, *71*, 644–648.

- (24) Mayr, S. I. Structure of a novel variant of cofactor F430. II. Proton inventory of methyl coenzyme M reductase. III. Further studies on the mode of action of F430. *ETH Zurich, ETH Dissertation 18549*, 2009; pp 138–211; <http://e-collection.library.ethz.ch/eserv/eth:323/eth-323-02.pdf>.
- (25) Scheller, S. Methyl-Coenzyme M Reductase: Mechanistic Studies with ^2H and ^{13}C Labels. *ETH Zurich, ETH Dissertation 19620*, 2011; pp 157–161; <http://e-collection.library.ethz.ch/eserv/eth:2974/eth-2974-02.pdf>.
- (26) Corresponding experiments will be reported separately, together with proton inventory studies on methane formation.
- (27) Singleton, D. A.; Thomas, A. A. *J. Am. Chem. Soc.* **1995**, *117*, 9357–9358.
- (28) Melander, L.; Saunders, W. H., Jr. *Reaction Rates of Isotopic Molecules*; Wiley: New York, 1980.
- (29) A small amount of $^{12}\text{CH}_3\text{D}$ is expected to be formed from the forward conversion of $^{12}\text{CH}_3\text{-S-CoM}$ (11% of the total remaining Me-S-CoM after 32 min) formed by activation of $^{12}\text{CH}_4$. Because the rates of methane formation and methane activation are the same under equilibrium conditions (~ 2000 times slower than methane formation in the initial seconds), and the $^{12}\text{CH}_3\text{-S-CoM}$ has to build up first via methane activation before it can be reconverted to $^{12}\text{CH}_3\text{D}$, the amount of $^{12}\text{CH}_3\text{D}$ formed along this path is comparable to the estimated error of detection, as confirmed by a full kinetic simulation of the system, which predicts that the $^{12}\text{CH}_3\text{D}$ formed from the 1% of unlabeled starting Me-S-CoM in the first 30 s increases by $\sim 20\%$ within 32 min due to this double turnover.
- (30) Chen, S.-L.; Blomberg, M. R. A.; Siegbahn, P. E. M. *Chem.—Eur. J.* **2012**, *18*, 6309–6315.
- (31) Pelmenchikov, V.; Siegbahn, P. E. M. *J. Biol. Inorg. Chem.* **2003**, *8*, 653–662.
- (32) Chen, S.-L. Beijing Institute of Technology; Siegbahn, P. E. M. Stockholm University. Personal communication.
- (33) Zavitsas, A. A.; Seltzer, S. *J. Am. Chem. Soc.* **1964**, *86*, 1265–1267.
- (34) Zavitsas, A. A.; Seltzer, S. *J. Am. Chem. Soc.* **1964**, *86*, 3836–3840.
- (35) Pryor, W. A.; Kneipp, K. G. *J. Am. Chem. Soc.* **1971**, *93*, 5584–5586.
- (36) Jaun, B. *Helv. Chim. Acta* **1990**, *73*, 2209–2217.
- (37) Li, X. H.; Telsler, J.; Kunz, R. C.; Hoffman, B. M.; Gerfen, G.; Ragsdale, S. W. *Biochemistry* **2010**, *49*, 6866–6876.
- (38) Dey, M.; Telsler, J.; Kunz, R. C.; Lees, N. S.; Ragsdale, S. W.; Hoffman, B. M. *J. Am. Chem. Soc.* **2007**, *129*, 11030–11032.
- (39) Yang, N.; Reiher, M.; Wang, M.; Harmer, J.; Duin, E. C. *J. Am. Chem. Soc.* **2007**, *129*, 11028–11029.
- (40) Westaway, K. C. In *Advances in Physical Organic Chemistry*; Richard, J. P., Ed.; Academic Press: New York, 2006; Vol. 41, pp 217–273.
- (41) Habibzadeh, S.; Rashidi, M.; Nabavizadeh, S. M.; Mahmoodi, L.; Hosseini, F. N.; Puddephatt, R. J. *Organometallics* **2009**, *29*, 82–88.
- (42) Jaun, B.; Pfaltz, A. *J. Chem. Soc., Chem. Commun.* **1988**, 293–294.
- (43) Lin, S. K.; Jaun, B. *Helv. Chim. Acta* **1992**, *75*, 1478–1490.
- (44) Gómez-Gallego, M.; Sierra, M. A. *Chem. Rev.* **2011**, *111*, 4857–4963.
- (45) Periana, R. A.; Bergman, R. G. *J. Am. Chem. Soc.* **1986**, *108*, 7332–7346.
- (46) Jones, W. D. *Acc. Chem. Res.* **2003**, *36*, 140–146.
- (47) Romeo, R.; Minniti, D.; Lanza, S. *J. Organomet. Chem.* **1979**, *165*, C36–C38.
- (48) Romeo, R.; Minniti, D.; Lanza, S.; Uguagliati, P.; Belluco, U. *Inorg. Chem.* **1978**, *17*, 2813–2818.
- (49) Tenn, W. J.; Young, K. J. H.; Oxgaard, J.; Nielsen, R. J.; Goddard, W. A.; Periana, R. A. *Organometallics* **2006**, *25*, 5173–5175.
- (50) Thompson, M. E.; Baxter, S. M.; Bulls, A. R.; Burger, B. J.; Nolan, M. C.; Santarsiero, B. D.; Schaefer, W. P.; Bercau, J. E. *J. Am. Chem. Soc.* **1987**, *109*, 203–219.
- (51) Goenrich, M.; Duin, E. C.; Mahlert, F.; Thauer, R. K. *J. Biol. Inorg. Chem.* **2005**, *10*, 333–342.
- (52) Kern, D. I.; Goenrich, M.; Jaun, B.; Thauer, R. K.; Harmer, J.; Hinderberger, D. *J. Biol. Inorg. Chem.* **2007**, *12*, 1097–1105.
- (53) Kunz, R. C.; Horng, Y.-C.; Ragsdale, S. W. *J. Biol. Chem.* **2006**, *281*, 34663–34676.
- (54) Mahlert, F.; Bauer, C.; Jaun, B.; Thauer, R. K.; Duin, E. C. *J. Biol. Inorg. Chem.* **2002**, *7*, 500–513.
- (55) Pabis, A.; Kaminski, R.; Ciepielowski, G.; Jankowski, S.; Paneth, P. *J. Org. Chem.* **2011**, *76*, 8033–8035.
- (56) Duan, Z. H.; Mao, S. D. *Geochim. Cosmochim. Acta* **2006**, *70*, 3369–3386.
- (57) Mahlert, F.; Grabarse, W.; Kahnt, J.; Thauer, R. K.; Duin, E. C. *J. Biol. Inorg. Chem.* **2002**, *7*, 101–112.
- (58) Duin, E. C.; Prakash, D.; Brungess, C. In *Methods in Methane Metabolism, Part A*; Rosenzweig, A. C., Ragsdale, S. W., Eds.; Methods in Enzymology, Vol. 494; Elsevier; Academic Press, Inc.: San Diego, 2011; pp 159–187.
- (59) Noll, K. M.; Donnelly, M. I.; Wolfe, R. S. *J. Biol. Chem.* **1987**, *262*, 513–515.